Regulation of Sar1 NH_2 terminus by GTP binding and hydrolysis promotes membrane deformation to control COPII vesicle fission

Anna Bielli,[1] Charles J. Haney,[1] Gavin Gabreski,[1] Simon C. Watkins,[1] Sergei I. Bannykh,[2] and Meir Aridor[1]

[1]Department of Cell Biology and Physiology, University of Pittsburgh School of Medicine, Pittsburgh, PA 15261
[2]Department of Pathology, Yale University School of Medicine, New Haven, CT 06520

The mechanisms by which the coat complex II (COPII) coat mediates membrane deformation and vesicle fission are unknown. Sar1 is a structural component of the membrane-binding inner layer of COPII (Bi, X., R.A. Corpina, and J. Goldberg. 2002. *Nature*. 419:271–277). Using model liposomes we found that Sar1 uses GTP-regulated exposure of its NH_2-terminal tail, an amphipathic peptide domain, to bind, deform, constrict, and destabilize membranes. Although Sar1 activation leads to constriction of endoplasmic reticulum (ER) membranes, progression to effective vesicle fission requires a functional Sar1 NH_2 terminus and guanosine triphosphate (GTP) hydrolysis. Inhibition of Sar1 GTP hydrolysis, which stabilizes Sar1 membrane binding, resulted in the formation of coated COPII vesicles that fail to detach from the ER. Thus Sar1-mediated GTP binding and hydrolysis regulates the NH_2-terminal tail to perturb membrane packing, promote membrane deformation, and control vesicle fission.

Introduction

Membrane fusion at constricted vesicle necks is required to detach vesicles from donor membranes, leading to vesicle fission. Repulsive hydration forces arising from water tightly bound to lipid head groups restrict membrane fusion. Defects in lipid packing that expose the hydrophobic interiors of bilayers generate molecular attractive forces between membranes that may overcome the repulsive forces and allow fusion. Such defects can arise from local changes in lipid composition and insertion/deinsertion of hydrophobic amino acid stretch that can induce extreme membrane curvature (Chernomordik and Kozlov, 2003). We hypothesize that cytosolic proteins use amphipathic domains with defined hydrophobic and hydrophilic faces to catalyze membrane deformation and fission. Upon membrane binding, the hydrophilic face of the amphipathic domains lie close to the charged head groups of phospholipids whereas the hydrophobic faces are embedded within the membrane interior and perturb fatty acid packing, thus deforming the membrane. The coat complex II (COPII) coat mediates export from the ER and has intrinsic vesicle fission capability (Matsuoka et al., 1998). The inner layer of COPII, composed of the small GTPase Sar1, Sec23, and Sec24 subunits, contacts the membrane (Bi et al., 2002). Sar1 contains an amphipathic domain in its extended NH_2 terminus, required for coat–membrane attachment. We analyzed the role of Sar1 and its GTP-regulated NH_2-terminal amphipathic domain in catalyzing membrane deformation and vesicle fission.

Results and discussion

Fig. 1 A shows the first 18 amino acids of the amphipathic tail of hamster Sar1a when presented on a helical wheel diagram. The charge distribution (12–6) with five of the polar residues clustered at the same helical plane, suggests that the tail can function as membrane destabilizer. To test the effects of Sar1 amphipathic domain on membrane stability, we incubated GST protein, or a GST protein fused to Sar1 amphipathic domain encompassing amino acid 1 to 26 (GST-Sar1-N-Tail) with spherical and uniform liposomes, sized at 100 nm by filter extrusion and verified by light scattering and EM. Protein effects on membrane stability were reported by changes in liposome morphology, as visualized by EM. Although GST protein alone did not affect liposome morphology, incubations with GST-Sar1-N-Tail destabilized the liposomes such that no ovoid membranes remained

Correspondence to M. Aridor: aridor@pitt.edu

Abbreviations used: COPII, coat complex II; DLPA, dilauryl-phosphatidic acid; DOPC, dioleyl-phosphatidyl choline; DTSSP, 3,3′-dithio-bis-sulfosuccinimidyl propionate; GAP, GTPase-activating protein; VSV-G, vesicular stomatitis virus glycoprotein.

The online version of this paper contains supplemental material.

The Journal of Cell Biology, Vol. 171, No. 6, December 19, 2005 919–924
http://www.jcb.org/cgi/doi/10.1083/jcb.200509095

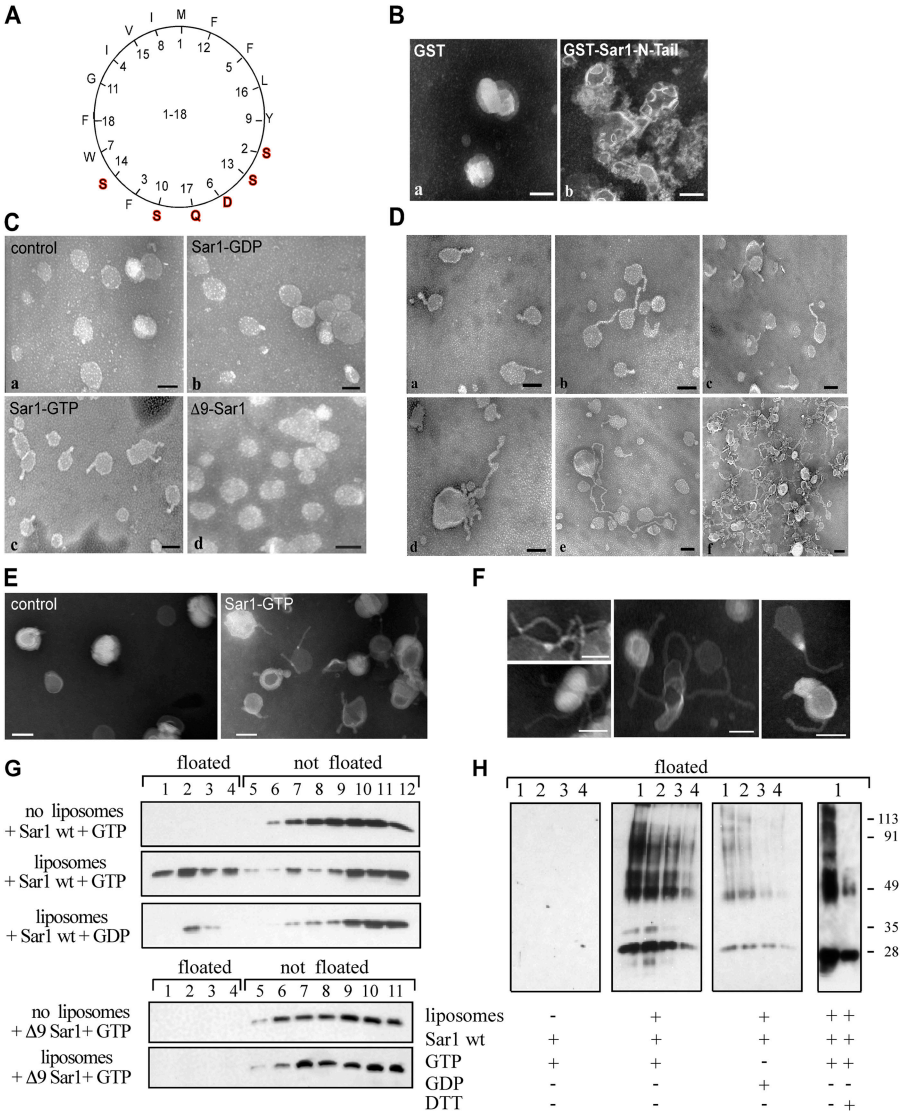

Figure 1. **Sar1 is capable of constricting lipid bilayers.** (A) Helical wheel representation of amino acids 1–18 of the NH_2 terminus of hamster Sar1a. (B) The NH_2-terminal tail of Sar1 destabilizes lipid membranes. Liposomes (100–120 nm, DOPC/DLPA, 80/20 mol percent) were incubated with 10 μM GST (a) or with 10 μM GST-Sar1-N-Tail (b) at 37°C for 1 h. At the end of incubations, liposomes were absorbed on charged grids and negatively stained with 1% phosphotungstic acid for EM analysis. (C) Sar1-GTP is capable of constricting liposome membranes. Liposomes (80–100 nm, DOPC and DLPA, 80/20 mol percent) were incubated in buffer (control; a), 10 μM Sar1-GDP (Sar1-T39N, b), 15 μM Sar1-GTP (Sar1-H79G, c), or 10 μM Δ9-Sar1 (d) mutants with GTP or GDP for 1 h at 37°C. Liposomes were stained and analyzed by EM. (D) A gallery of Sar1-GTP–induced tubulating (a–d) and fused (e and f) DOPC/DLPA liposomes. (E) Cholesterol/DOPC/DLPA (20/75/5 mol percent) liposomes (100–120 nm) were incubated as described above in the absence or presence of Sar1-GTP as indicated. (F) A gallery of tubulating cholesterol/DOPC/DLPA liposomes deformed during incubations with Sar1-GTP. Bars, 100 nm. (G) Sar1 uses its amphipathic NH_2 terminus to bind liposomes in a GTP-dependent manner. Sar1 wt (1 μg) or Δ9-Sar1 (1 μg) was incubated with GTP or GDP in the absence or presence of liposomes as indicated. Liposomes were floated into a sucrose gradient and fractions collected from the top were numbered sequentially and analyzed by Western blot with Sar1 antibody. Fractions 1–4 contain liposome-associated Sar1, whereas fractions 5–12 contain unbound Sar1. (H) Liposome-bound Sar1 GTP can form lateral protein interactions. Liposome-bound Sar1 wt (1 μg) was cross-linked with DTSSP (100 μM) and loaded onto sucrose gradients as in G. Floated fractions were analyzed on nonreducing gels by Western blotting. When indicated, DTT (50 mM) was added to reverse cross-linking.

and fragmented disorganized membranes were visible (Fig. 1 B, a and b). Therefore, the NH_2 terminus of Sar1 is capable of destabilizing lipid bilayers. We next analyzed whether GTP loading on Sar1 can regulate the membrane-destabilizing activity of the Sar1 NH_2 terminus. In the absence of Sar1, liposomes appeared as uniformly sized spheres as observed in incubations with GST (Fig. 1 C, a). This morphology was unchanged when liposomes were incubated with Sar1 mutant that is deficient in GTP binding, (Sar1-GDP [T39N]; Fig. 1 C, b). In contrast, liposome morphology was markedly modified when liposomes were incubated with a constitutively active mutant of Sar1 that cannot hydrolyze GTP (Sar1-GTP [H79G]; Aridor et al., 1995) (Fig. 1, C [c], E, and gallery in D and F). Short tubules were seen emanating from the liposomes (Fig. 1 D, a–d), as well as longer tubular structures (Fig. 1, D [e] and F), which sometimes developed to form extended networks of tubular membranes (Fig. 1 D, f). Formation of elongated structures with extended membrane surface is likely due to fusion of smaller ovoid liposome membranes (refer to Fig. 1 D, e, for examples of intermediates in liposome fusion). Initiation of liposome tubulation was detected with Sar1-GTP at 4 μM (unpublished data). Therefore, the activity of Sar1 NH_2 terminus depends on Sar1 activation. Furthermore, this activity is dependent on the presence of intact NH_2 terminus. A GTP-loaded truncated form of Sar1 with the proximal nine amino acids of the NH_2 terminus removed (Δ9-Sar1) failed to destabilize or tubulate liposomes (Fig. 1 C, d). Δ9-Sar1 can bind and hydrolyze GTP but cannot interact efficiently with membranes (Huang et al., 2001). We separated liposome bound Sar1 from unbound protein on sucrose density gradients to analyze Sar1 interaction with liposomes. As observed morphologically, Sar1 interactions with liposomes were dependent on GTP binding and intact NH_2 terminus amphipathic domain (Fig. 1 G). High molecular weight products of Sar1 suggestive of oligomerization were observed when liposome bound Sar1 was cross-linked with reversible cross-linker (3,3′-dithio-bis-sulfosuccinimidyl propionate [DTSSP]; Fig. 1 H), and these products were reduced to mostly monomeric (~25 kD) protein by DTT. It is possible that the high concentrations of membrane-recruited Sar1 supported lateral protein interactions on the liposome surface, and these interactions may have further promoted local

perturbation of lipid packing and membrane constriction. High concentrations of Sar1 are observed on tubules formed on ER membranes (Aridor et al., 2001).

Having established that Sar1 can use its tail not only for membrane attachment but also as a GTP-regulated membrane–deforming machine, we investigated the role of this activity in vesicle fission. In previous studies we demonstrated that activation of Sar1 in permeabilized cells, in the absence of COPII subunits led to Sar1-induced tubulation and constriction of ER exit sites (Aridor et al., 2001). These tubules were reminiscent of intermediates in vesicle fission. COPII subunits, which subsequently bind Sar1 may organize the vesicle cage to restrict membranes for fission, and provide the GTPase-activating protein (GAP) activity that controls the interaction of Sar1 amphipathic domain with constricted membranes. Thus GTP hydrolysis may facilitate the progression from Sar1-induced membrane constriction to vesicle fission. We tested the role of GTP hydrolysis in regulating vesicle release. When added together with cytosol to permeabilized cells, Sar1-GTP inhibited the synchronous export of the model cargo protein vesicular stomatitis virus glycoprotein (VSV-G) tsO45 from the ER (as analyzed by immunofluorescence). The resulting morphology was suggestive of intermediates in vesicle formation that are arrested at the membrane constriction and fission stage (Fig. S 1, h, i, q, and r available at http://www.jcb.org/cgi/content/full/jcb.200509095/DC1). To focus on vesicle release, we used a biochemical assay that reconstitutes COPII vesicle formation from ER microsomes expressing ts045 VSV-G. ER membranes were separated from the vesicular fraction using differential centrifugation to monitor Sar1-dependent mobilization of cargo proteins from the ER. As previously characterized, ER membranes incubated with cytosol in the presence of increasing concentrations of Sar1-GTP produced normal COPII-coated vesicles selectively enriched in VSV-G and an endogenous cargo, the SNARE protein Bet1 (Fig. 2 A, lanes 3–5; Rowe et al., 1996; Aridor et al., 1998). Budding was abolished in incubations with cytosol and Sar1-GDP (Fig. 2 A, lane 6, see quantitation of all panels in Fig. 2 D). Although this assay did not reproduce the budding arrest observed by immunofluorescence, the assay used a trituration step originally included to facilitate the separation of vesicles from donor membranes. This step might physically promote the shearing of vesicles connected by membranes already constricted by Sar1-GTP (Fig. 1). Omitting the trituration step from the budding assay enhanced the efficiency of the budding reaction under control conditions. Incubation of VSV-G–containing membranes with cytosol led to efficient mobilization of VSV-G and Bet1 from the ER (Fig. 2, lanes 2 in B and C, and compare with lane 2 in A) and budding was inhibited by Sar1-GDP (Fig. 2 B [lane 6] and C [lane 7]). However, incubating membranes in the presence of Sar1-GTP now blocked budding of VSV-G and Bet1 from the ER (Fig. 2 B, lanes 3–5). Incubating membranes with similar concentrations of wild-type Sar1 did not affect budding (Fig. 2 C, lanes 3–6). Therefore, we could reproduce the Sar1-GTP–induced ER export arrest observed by immunofluorescence in a vesicle formation assay suggesting that inhibition is exerted at the level of vesicle release.

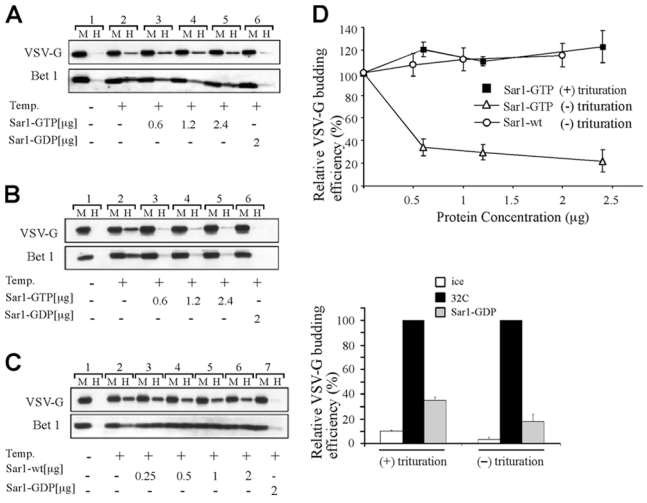

Figure 2. **Sar1-GTP (H79G) inhibits vesicle release.** (A) tsO45-VSV-G–containing membranes were incubated (40 μl final volume) in the presence of cytosol for 30 min on ice (lane 1) or at 32°C (lanes 2–6) in the absence (lanes 1 and 2) or presence of Sar1-GTP (lanes 3–5) or Sar1-GDP (lane 6). At the end of incubation, membranes were subjected to a physical trituration step. The vesicle fraction (H) was separated from the donor membranes (M) by differential centrifugation and analyzed by Western blotting with antibodies against VSV-G and the SNARE protein Bet1. (B and C) The budding assay was performed as above without physical trituration. The mobilization of VSV-G and Bet1 to the vesicular fraction was analyzed in the presence of increasing concentrations of either Sar1-GTP (B, lanes 3–5) or Sar1 wt (C, lanes 3–6) as indicated. (D) Quantitation of the budding efficiency for VSV-G in three independent experiments under the indicated conditions is shown (means ± SEM).

Several reasons could account for the inhibition of vesicle release by Sar1-GTP. Addition of exogenous excess Sar1 may create a stoichiometric imbalance between COPII components, inhibiting proper vesicle coating, formation, and release. We therefore tested whether constitutive activation of endogenous cytosolic Sar1 protein affected vesicle release. We used a nonhydrolyzable analogue of GTP, GTP-γ-S, to activate cytosolic Sar1. Similar to the results obtained with Sar1-GTP, GTP-γ-S inhibited vesicle release (Fig. 3 A, lanes 3–7, and B, lane 3). Irreversible binding of Sar1 to membranes could prevent vesicle uncoating depleting coat components needed for budding. However, the abundance of residual-free COPII (as analyzed by Sec23 levels) remained largely unchanged under conditions that inhibited vesicle release (Fig. 3 B). It is possible that inhibition of Sar1-mediated GTP hydrolysis inhibits cargo selection, yet release of vesicles, which remain coated due to the inhibition of GTP hydrolysis, progresses normally. We thus analyzed whether cargo-depleted COPII-coated vesicles are generated in incubations with Sar1-GTP-γ-S by analyzing the vesicular fraction on sucrose gradients. We found VSV-G– and Bet1-containing vesicles that retained coat components (identified using Sec23 antibody) in control (32°C) incubations, but not in similar incubations performed with GTP-γ-S (Fig. 3 C). Therefore cargo-depleted COPII vesicles are not released under these conditions. Indeed, GTP hydrolysis is not required for efficient cargo selection, as observed during the formation of Sar1-GTP–stabilized cargo selective prebudding complexes (Aridor et al., 1998; Kuehn et

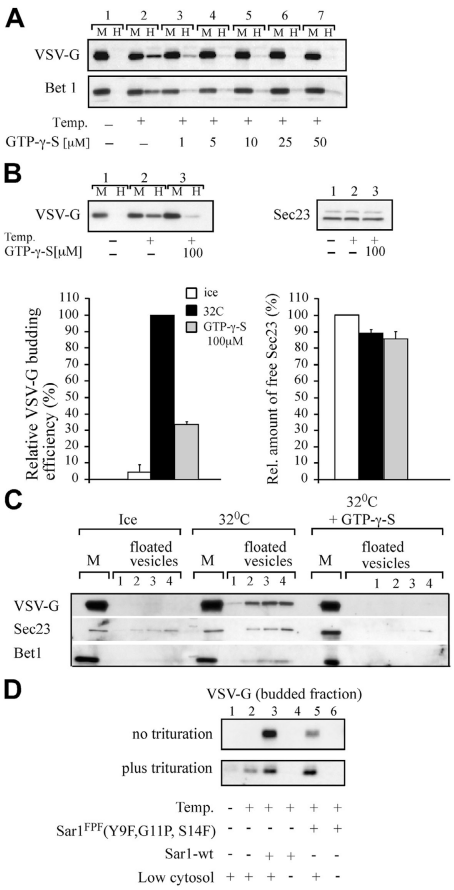

Figure 3. **Vesicle release is regulated by endogenous Sar1 GTPase activity and requires functional NH_2-terminal amphipathic domain.** (A) Inhibition of endogenous Sar1 GTPase activity inhibits COPII vesicle release. VSV-G–containing membranes were incubated in the presence of cytosol for 30 min on ice (lane 1) or at 32°C (lanes 2–7) in the absence (lanes 1 and 2) or presence of increasing concentrations of GTP-γ-S as indicated. At the end of incubation, the vesicle fraction (H) was separated from the donor membranes (M) by differential centrifugation without trituration and analyzed by Western blotting as indicated. (B) COPII components are not limiting under conditions inhibitory to vesicle release. The vesicle formation reaction was carried in the absence or presence of GTP-γ-S (100 μM). At the end of incubation the vesicle fraction was separated from the membrane fraction. The supernatant of the vesicle fraction was collected and analyzed for available COPII component Sec23. Quantitation of the amount of VSV-G in the vesicle fraction (left) and COPII Sec23 subunit remaining in the supernatant of the vesicle fraction (right) averaged from three independent experiments ± SEM. (C) Cargo-free COPII vesicles are not produced when Sar1 GTPase activity is inhibited. Vesicles generated as described in A, in the presence or absence of 100 μM GTP-γ-S, were separated from donor membranes by centrifugation and floated into sucrose gradients. Fractions 1–4 (collected from the top of the gradient) contain floated vesicles (VSV-G– and Bet1-containing fractions). The presence of VSV-G, Sec23, and Bet1 in the vesicle fraction was determined as indicated. (D) $Sar1^{FPF}$ (Y9F, G11P, S14F) does not support efficient vesicle release. In the upper panel, VSV-G–containing membranes were incubated (40 μl final volume) with limiting cytosol in the presence of Sar1 wt or $Sar1^{FPF}$ (2.5 μg each) on ice or at 32°C for 30 min as indicated. At the end of incubation the vesicle fraction was prepared without physical trituration and analyzed by Western blotting. For the trituration assay (lower panel), membranes were incubated (40 μl final volume) with limiting cytosol in the presence of Sar1 wt or $Sar1^{FPF}$ (2 μg each) for 15 min on ice or at 32°C as indicated. The vesicle fraction was prepared with physical trituration and analyzed by Western blotting.

al., 1998), or in budding assays carried in the presence of Sar1-GTP that included physical trituration (Fig. 2 A).

GTP binding and hydrolysis by Sar1 regulates the interactions of Sar1 amphipathic domain with membranes (Fig. 1). We tested the role of the amphipathic domain in vesicle release, by generating a mutant with reduced flexibility and enhanced hydrophobic face, $Sar1^{FPF}$ (Y9F, G11P, and S14F). Although reducing the hydrophobic content of Sar1 NH_2 terminus by replacement of bulky hydrophobic residues with hydrophilic residues or by truncations inhibited function by inhibiting membrane binding (Huang et al., 2001), $Sar1^{FPF}$ was functional in directing coat assembly on ER membranes in a GTP-dependent manner (Fig. S2 and supplemental text available at http://www.jcb.org/cgi/content/full/jcb.200509095/DC1). Sar1 is not simply used as a stoichiometric component of COPII during vesicle formation. Budding reactions carried with low cytosol concentrations were dependent on exogenously added Sar1 (Fig. 3 D, lanes 2–4, upper and lower panels; Aridor et al., 1998). We used this condition to test the ability of $Sar1^{FPF}$ to support vesicle fission. Despite its functionality in coat assembly, the mutant was less efficient in supporting vesicle release in a nontriturated fission reporting budding assay when compared with wild-type Sar1 (Fig. 3 D, compare lanes 3 to 5, upper panel). We found that $Sar1^{FPF}$ consistently exhibited only 30–40% budding activity when compared with wild type under various incubation conditions (unpublished data). In contrast, $Sar1^{FPF}$ was as active as wild-type Sar1 in supporting the budding reaction when trituration was introduced to analyze fission-independent vesicle budding activity (Fig. 3 D, lower panel, compare lanes 3 and 5). Thus, $Sar1^{FPF}$ supported coat assembly and vesicle formation, yet the altered amphipathic domain led to a deficiency in vesicle release.

The nonhydrolyzable GTP analogue GppNHp can replace GTP in supporting COPII-mediated vesicle fission in yeast (Barlowe et al., 1994) and did not inhibit vesicle release mediated by mammalian COPII (Fig. S3 available at http://www.jcb.org/cgi/content/full/jcb.200509095/DC1). Unlike GTP-γ-S, GppNHp does not stabilize Sar1 in activated transition state (Bi et al., 2002), and was inefficient in stabilizing Sar1 interactions with ER membranes (Fig. S3 and supplemental text available at http://www.jcb.org/cgi/content/full/jcb.200509095/DC1). The conformation dynamics allowed by GppNHp may promote and destabilize Sar1 interactions with membranes sufficiently to support vesicle fission.

By following the mobilization of cargo proteins we demonstrate that when Sar1 is stabilized in its active state, coated COPII vesicles fail to detach from the ER. We visualized COPII vesicles generated in the presence of Sar1-GTP (Fig. 4, a–d) or GTP-γ-S (Fig. 4, e and f) and cytosol in permeabilized NRK cells using EM (Fig. 4, a–f). COPII vesicles were identified using gold immunolabeling to detect both the inner (Sar1 and Sec23; Fig. 4, a–c) and outer (Sec13 and Sec31; Fig. 4, d–f) layers of the COPII coat. We observed beads on a string like 60–80 nm vesicles generated at ER exit sites (Bannykh et al., 1996). We now demonstrate that these vesicles are COPII-coated vesicles that fail to detach from the ER. Mammalian COPII vesicles seem similar to yeast COPII vesicles (Barlowe et al., 1994).

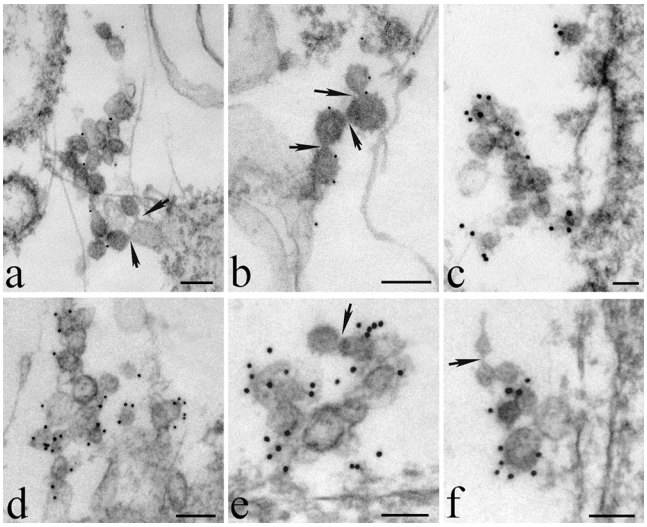

Figure 4. **Inhibition of GTP hydrolysis by Sar1 leads to the formation of COPII-coated vesicles that fail to detach from the ER.** NRK cells were permeabilized and incubated (200 μl final volume) in the presence of Sar1-GTP (5 μg, a–d) or GTP-γ-S (100 μM, e and f) and cytosol as described previously (Bannykh et al., 1996). At the end of incubation the cells were fixed and incubated with primary antibodies to Sar1, Sec23, Sec13, and Sec31 and protein A (5 nm, a, b, and d) or (10 nm, c, e, and f) conjugates. The cells were postfixed, stained, and embedded in Epon. 70 nm sections were analyzed by transmission EM. Clusters of 60 nm vesicles were formed in the presence of Sar1-GTP and cytosol. These vesicles contained both inner (Sar1 in a and b and Sec23 in c) and outer (Sec13 in d and Sec31 in e and f) COPII layers. Arrows indicated membrane continuity between the vesicles themselves and between vesicles and ER membranes. Bars, 100 nm.

The vesicles appeared coated and assembled yet clear constricted membrane connections between the coated vesicles themselves and the ER membrane were visible (Fig. 4, a–f, see arrows).

We propose a model to describe the role of Sar1 in catalyzing membrane deformation and fission. Sar1 amphipathic domain is inserted in the bilayer upon GTP binding, inducing membrane curvature and constriction. COPII assembly into 60–80 nm cages that bind acidic lipid headgroups may increase membrane tension and define optimal sites for membrane fission (Matsuoka et al., 1998; Pathre et al., 2003). Membrane curvature generated at the vesicle neck may regulate COPII GAP activities to promote GTP hydrolysis. GTP hydrolysis will result in Sar1 removal repositioning the coat for final constriction of the relived vesicle neck, while further disrupting local lipid packing to facilitate fission. Cargo proteins regulate GTP hydrolysis by Sar1 (Sato and Nakano, 2004) raising the possibility that cargo selection is coupled to COPII vesicle fission.

Our results suggest that GTP-regulated interactions of Sar1 with membranes through the amphipathic domain, provide a mechanism to deform membranes. In a recent related work, yeast Sar1 was also shown to use its NH_2-terminal helix to deform membranes and support vesicle release (Lee et al., 2005). Our results further demonstrate that GTP hydrolysis is required to control and promote the fission reaction. Amphipathic domains may be similarly used to catalyze vesicle fission throughout the endocytic and secretory pathways as observed for epsin (Ford et al., 2002), amphiphysins (Yoshida et al., 2004), and perhaps members of the ARF/ARF GAP families.

Materials and methods

Hamster Sar1a wild-type, H79G, T39N, and Sar1^{FPF} mutant proteins were purified as described previously (Rowe et al., 1996). GST proteins (GST, GST-Sar1-GTP, and GST-Sar1-N-tail) were purified using the bulk GST purification protocol (Amersham Biosciences). GST-Sar1 was mutated to generate GST-Sar1-N-tail, and Sar1a wt was mutated to generate Sar1 S14F Y9F G11P using Quickchange mutagenesis kit (Stratagene). Mutagenesis was verified by sequencing. Rat liver cytosol was prepared as previously described (Aridor et al., 1995). Antibodies to COPII components, VSV-G, and Bet1 were a gift from Dr. W.E. Balch (The Scripps Research Institute, La Jolla, CA). Dioleyl-phosphatidyl choline (DOPC) and dilauryl-phosphatidic acid (DLPA) were purchased from Avanti Polar Lipids, Inc. DTSSP was from Pierce Chemical Co. and digitonin was from Wako. Other reagents were from Sigma-Aldrich.

Infection of NRK cells
NRK cells were infected with tsO45 VSV as described previously (Aridor et al., 1995).

Preparation of membrane microsomes
Microsomes from VSV-infected or -uninfected NRK cells were prepared as described previously (Rowe et al., 1996).

Coat recruitment assay
Sec23 recruitment assays were performed as described previously (Pathre et al., 2003). For recruitment assays with GTS-γ-S or GppNHp, GTP was omitted from the reaction. At the end of incubation, the reactions were loaded on and centrifuged through a 15% sucrose cushion (Pathre et al., 2003). For two stage recruitment assays, membranes were incubated as above, washed, resuspended, and incubated in a second stage incubation in the presence of cytosol for 15 min at 32°C. At the end of incubation, the membranes were diluted and washed with 25 mM Hepes (pH 7.2), 250 mM sorbitol, 2.5 mM $Mg(OAc)_2$ and 250 mM KOAc, resuspended in 25 mM Hepes, pH 7.2, 250 mM sorbitol, 2.5 mM $Mg(OAc)_2$ and 250 mM KCl, and centrifuged through a 15% sucrose cushion (Pathre et al., 2003).

ER vesicle budding assay
COPII budding assays were performed as described previously (Rowe et al., 1996). VSV-G or Bet1 in vesicle and donor membrane fractions were measured by SDS-PAGE and quantitative Western blotting. For analysis of budding in the presence of GTS-γ-S or GppNHp, GTP was omitted from the incubations. For nontrituration vesicle formation assays, VSV-G–expressing microsomes were incubated as described previously (Rowe et al., 1996). At the end of incubation, the membranes were directly sedimented by brief centrifugation with no further treatment (16,000 *g*, 3 min at 4°C) and the supernatant containing the vesicle fraction was collected by centrifugation (186,000 *g*, 20 min at 4°C). The vesicle and donor membrane fractions were analyzed for VSV-G and Bet-1. The percent of VSV-G in the vesicular fraction was calculated from the total amount of VSV-G in vesicle and donor membranes for each sample. For presentation budding in control samples was set to 100%.

Vesicle isolation by floatation
Donor membranes were separated from the vesicle fraction as described above. The vesicle fraction (50 μl) was mixed with 150 μl of 1.65 M sucrose in liposome buffer (20 mM Hepes, pH 7.2, 150 mM KOAc, and 250 mM sorbitol) and layered with 150μl of 0.75 M sucrose and 20 μl of buffer. Samples were centrifuged at 367,500 *g* for 90 min at 4°C. Fractions were collected from the top of the gradient, separated by SDS page, and analyzed using Western blots.

Semiintact cell morphological analysis and microscopy
VSV-infected NRK cells were permeabilized and ER export was reconstituted as described previously (Aridor et al., 1995). For two stage assays, permeabilized cells were incubated in the presence of GTP-γ-S, Sar1 proteins, and ATP regeneration system. At the end of incubation, the cells were washed twice with buffer containing 25 mM Hepes, pH 7.2, 110 mM KOAc and 1 mM $Mg(OAc)_2$, and incubated with cytosol and ATP regeneration system to reconstitute COPII recruitment, fixed with 3% paraformaldehyde, and processed for immunofluorescence (Aridor et al., 2001). Fluorescence images were acquired on a confocal microscope (Fluoview 500; Olympus).

Liposome preparation for morphological and biochemical experiments
A lipid film was formed by drying chloroform stock solutions of cholesterol, DOPC, and DLPA in glass tubes. For morphological analysis, a stock

of 80 mol percent DOPC and 20 mol percent DLPA, or cholesterol, DOPC, and DLPA (20/75/5 mol percent, respectively) were dried and hydrated in 20 mM Hepes, pH 7.2, 25 mM KCl, 150 mM K-glutamate, 2.5 mM $Mg(OAc)_2$ at 37°C with occasional vortex mixing for 45 min. The resulting liposome suspension was freeze thawed for three to five times and extruded sequentially through polycarbonate filters of 400 and 80 nm pore size (Avanti Polar Lipids, Inc.). The size distribution and purity of extruded liposomes was verified by dynamic light scattering and EM. Liposomes were used at a final concentration of 250 μg/ml.

For biochemical analysis, DOPC/DLPA (95/5 mol percent) were hydrated in liposome buffer and extruded through a 400-nm polycarbonate filter. A pure population of 180–220 nm diam liposomes were generated and used at a final concentration of 400 μM.

Immuno-EM

Immuno-EM was carried as previously described (Bannykh et al., 1996).

Negative stain and morphological analysis of liposomes

Liposomes, prepared as described above, were incubated in the presence of Sar1-GTP and GTP (1 mM), Sar1-GDP and GDP (2 mM), GST or GST-Sar1-N-Tail in a buffer containing 20 mM Hepes, pH 7.2, 25 mM KCl, 150 mM K-glutamate, 2.5 mM $Mg(OAc)_2$ for 1 h at 37°C. At the end of incubation, reactions were absorbed on charged grids for 10 min, stained with 1% PTA for 3–6 min, dried, and analyzed by EM. Representative pictures from at least two independent experiments are shown.

Sar1 binding to liposomes

Sar1 wt (1 μg) was incubated in buffer (liposome buffer) containing 20 mM Hepes, pH 7.0, 150 mM KOAc, 250 mM Sorbitol, 2.5 mM $Mg(OAc)_2$, 2.5 mM EDTA, and 2 mM of GTP or GDP as indicated, in the presence of 400 μM liposomes containing 95 mol percent DOPC and 5 mol percent DLPA at 26°C for 45 min at a final volume of 50 μl. At the end of the reaction, DTSSP was added to a final concentration of 100 μM and the reaction was incubated for 15 min at 26°C. Cross-linking was stopped by the addition of Tris-HCl (50 mM, pH 8.0). At the end of incubation, the resulting samples (52 μl) were mixed with 150 μl of 1.65 M sucrose in liposome buffer and layered with 150 μl of 0.75 M sucrose and 20 μl of buffer. Samples were centrifuged at 367,500 *g* for 90 min at 4°C. Fractions were collected from the top of the gradient separated on nonreducing gels and analyzed by Western blot with anti-Sar1 antibodies. Similar cross-linking patterns of Sar1 were obtained when cross-linking was carried after isolation of liposome-bound Sar1 from sucrose gradients. In addition, similar cross-linking pattern was obtained, when cross-linking was carried with noncleavable cross-linker BS^3 (1 mM) and incubations were carried in the presence of DTT (2.5 mM).

Online supplemental material

Fig. S1 depicts how Sar1-GTP inhibits the progression of VSV-G from the ER to vesicular tubular clusters. Fig. S2 illustrates that $Sar1^{FPF}$ (Y9F, G11P, S14F) is functional in mediating COPII assembly. In Fig. S3 we show how GppNHp is inefficient in stabilizing Sar1 binding to ER membranes. Online supplemental material is available at http://www.jcb.org/cgi/content/full/jcb.200509095/DC1.

We thank Drs. O.A. Weisz for critically reading the manuscript and W.G. Hill for technical advice.

The study was supported by National Institutes of Health grant DK 062318 (M. Aridor) and the Osteogenesis Imperfecta Foundation (A. Bielli).

Submitted: 16 September 2005
Accepted: 10 November 2005

References

Aridor, M., S. Bannykh, T. Rowe, and W.E. Balch. 1995. Sequential coupling between COPII and COPI vesicle coats in endoplasmic reticulum to Golgi transport. *J. Cell Biol.* 131:875–893.

Aridor, M., J. Weissman, S. Bannykh, C. Nuoffer, and W.E. Balch. 1998. Cargo selection by the COPII budding machinery during export from the ER. *J. Cell Biol.* 141:61–70.

Aridor, M., K.N. Fish, S. Bannykh, J. Weissman, T.H. Roberts, J. Lippincott-Schwartz, and W.E. Balch. 2001. The Sar1 GTPase coordinates biosynthetic cargo selection with endoplasmic reticulum export site assembly. *J. Cell Biol.* 152:213–229.

Bannykh, S.I., T. Rowe, and W.E. Balch. 1996. The organization of endoplasmic reticulum export complexes. *J. Cell Biol.* 135:19–35.

Barlowe, C., L. Orci, T. Yeung, M. Hosobuchi, S. Hamamoto, N. Salama, M.F. Rexach, M. Ravazzola, M. Amherdt, and R. Schekman. 1994. COPII: a membrane coat formed by Sec proteins that drive vesicle budding from the endoplasmic reticulum. *Cell.* 77:895–907.

Bi, X., R.A. Corpina, and J. Goldberg. 2002. Structure of the Sec23/24-Sar1 pre-budding complex of the COPII vesicle coat. *Nature.* 419:271–277.

Chernomordik, L.V., and M.M. Kozlov. 2003. Protein-lipid interplay in fusion and fission of biological membranes. *Annu. Rev. Biochem.* 72:175–207.

Ford, M.G.J., I.G. Mills, B.J. Peter, Y. Vallis, G.J.K. Praefcke, P.R. Evans, H.T. McMahon. 2002. Curvature of clathrin-coated pits driven by epsin. *Nature*. 419: 361–366.

Huang, M., J.T. Weissman, S. Beraud-Dufour, P. Luan, C. Wang, W. Chen, M. Aridor, I.A. Wilson, and W.E. Balch. 2001. Crystal structure of Sar1-GDP at 1.7 A resolution and the role of the NH_2 terminus in ER export. *J. Cell Biol.* 155:937–948.

Kuehn, M.J., J.M. Herrmann, and R. Schekman. 1998. COPII-cargo interactions direct protein sorting into ER-derived transport vesicles. *Nature.* 391:187–190.

Lee, M.C., L. Orci, S. Hamamoto, E. Futai, M. Ravazzola, and R. Schekman. 2005. Sar1p N-terminal helix initiates membrane curvature and completes the fission of a COPII vesicle. *Cell.* 122:605–617.

Matsuoka, K., L. Orci, M. Amherdt, S.Y. Bednarek, S. Hamamoto, R. Schekman, and T. Yeung. 1998. COPII-coated vesicle formation reconstituted with purified coat proteins and chemically defined liposomes. *Cell.* 93:263–275.

Pathre, P., K. Shome, A. Blumental-Perry, A. Bielli, C.J. Haney, S. Alber, S.C. Watkins, G. Romero, and M. Aridor. 2003. Activation of phospholipase D by the small GTPase Sar1p is required to support COPII assembly and ER export. *EMBO J.* 22:4059–4069.

Rowe, T., M. Aridor, J.M. McCaffery, H. Plutner, C. Nuoffer, and W.E. Balch. 1996. COPII vesicles derived from mammalian endoplasmic reticulum microsomes recruit COPI. *J. Cell Biol.* 135:895–911.

Sato, K., and A. Nakano. 2004. Reconstitution of coat protein complex II (COPII) vesicle formation from cargo-reconstituted proteoliposomes reveals the potential role of GTP hydrolysis by Sar1p in protein sorting. *J. Biol. Chem.* 279:1330–1335.

Yoshida, Y., M. Kinuta, T. Abe, S. Liang, K. Araki, O. Cremona, G. Di Paolo, Y. Moriyama, T. Yasuda, P. De Camilli, and K. Takei. 2004. The stimulatory action of amphiphysin on dynamin function is dependent on lipid bilayer curvature. *EMBO J.* 23:3483–3491.